Supporting Information for

H-bonding and C-H···π assisted mechanofluorochromism of triphenylamine-containing vinylheterocycles bearing cyano and methyl

Jiang Peng,[‡[a]] Jinyu Zhao,[‡[a]] Longde Zheng,[[a]] Kaiqi Ye,[[a]] Jingbo Sun,[[a]] Ran Lu*[[a]]

[a]State Key Laboratory of Supramolecular Structure and Materials, College of Chemistry, Jilin University, Changchun 130012, P. R. China

E-mail: luran@mail.jlu.edu.cn

Table S1 Photophysical data of the synthesized compounds in solutions.

Compound	Solvents	λ_{abs}[a]	λ_{em}[b]	$\Delta\nu_{st}$/ (cm^{-1})[c]	Φ_F[d]
BIT	Cyclohexane	302, 381	426, 443	2773	0.51
	Toluene	306, 387	444	3317	0.52
	THF	305, 383	454	4083	0.56
	Chloroform	305, 385	472	4788	0.26
	DMF	304, 388	490	5365	0.55
BITM	Cyclohexane	302, 388	433, 454	2679	0.66
	Toluene	305, 393	454	3419	0.57
	THF	304, 389	473	4565	0.66
	Chloroform	303, 396	496	5091	0.34
	DMF	305, 390	501	5681	0.71
BICT	Cyclohexane	302, 434	483, 511	2338	-
	Toluene	304, 439	513	3210	-
	THF	298, 427	529	4516	-
	Chloroform	299, 445	543	4056	-
	DMF	297, 422	575	6305	-
BICTM	Cyclohexane	301, 443	499	2533	-
	Toluene	301, 446	533	3589	-
	THF	297, 434	555	5023	-
	Chloroform	298, 453	581	4863	-
	DMF	297, 436	601	6297	-
BOTM	Cyclohexane	302, 402	447, 467	2504	0.34
	Toluene	303, 406	479	3753	0.49
	THF	302, 404	511	5183	0.46
	Chloroform	303, 409	521	5256	0.31
	DMF	302, 405	559	6802	0.17
BTTM	Cyclohexane	302, 408	453, 475	2434	0.34
	Toluene	302, 412	485	3653	0.38
	THF	301, 411	521	5137	0.32
	Chloroform	303, 415	529	5193	0.26
	DMF	303, 413	567	6576	0.20
BTCT	Cyclohexane	295, 444	491	2156	-
	Toluene	298, 451	530	3305	-
	THF	293, 448	553	4238	-
	Chloroform	298, 455	566	4310	-
	DMF	294, 452	611	5757	-
BTCTM	Cyclohexane	296, 454	512	2495	-
	Toluene	296, 460	554	3689	-
	THF	294, 457	590	4933	-
	Chloroform	296, 464	601	4913	-
	DMF	297, 460	625	5739	-

[a] Measured in solution (1×10^{-5} M), [b] Excited at 390 nm (**BIT** and **BITM**) and Excited at 430 nm (**BICT** and **BICTM**), Excited at 400 nm (**BOTM** and **BTTM**), Excited at 430 nm (**BTCT** and **BTCTM**), [c] $\Delta\nu_{st} = \nu_{abs} - \nu_{em}$, [d] The fluorescence quantum yield (Φ_F) was measured using 9,10-diphenylanthracene in toluene (0.1 M) (Φ_F = 0. 85) as standard.

Table S2 Single crystal data of **BICTM**, **BTTM** and **BTCT**.

	BICTM (C_2H_5OH)	**BTTM**	**BTCT**
Formula	$C_{32}H_{30}N_4O$	$C_{29}H_{24}N_2S$	$C_{56}H_{38}N_6S_2$
Formula weight	486.60	432.56	859.04
Space group	Pī	P2(1)/n	Pī
Crystal system	Triclinic	Monoclinic	Triclinic
a (Å)	7.8915(3)	22.5283(7)	10.7275(5)
b (Å)	12.9891(6)	5.7765(2)	13.9409(7)
c (Å)	13.8662(6)	19.8649(6)	16.1945(8)
α (deg)	69.849(2)	90.000	73.661(2)
β (deg)	89.757(2)	114.8520(10)	81.696(2)
γ (deg)	87.177(2)	90.000	72.068(2)
V (Å^3)	1332.59(10)	2345.72(13)	2206.76(19)
Z	2	4	2
D_{calc}(g/cm^3)	1.213	1.225	1.293
μ (mm^{-1})	0.075	0.157	0.168
Final R indices	R1 = 0.0465	R1 = 0.0499	R1 = 0.0472
[I>2sigma(I)]	wR2 = 0.1082	wR2 = 0.1184	wR2 = 0.1132
R indices(all data)	R1 = 0.0799 wR2 =0.1255	R1 = 0.0834 wR2 =0.1347	R1 = 0.0934 wR2 = 0.1431
GoF	1.048	1.051	1.030
CCDC	1851499	1851402	1851401

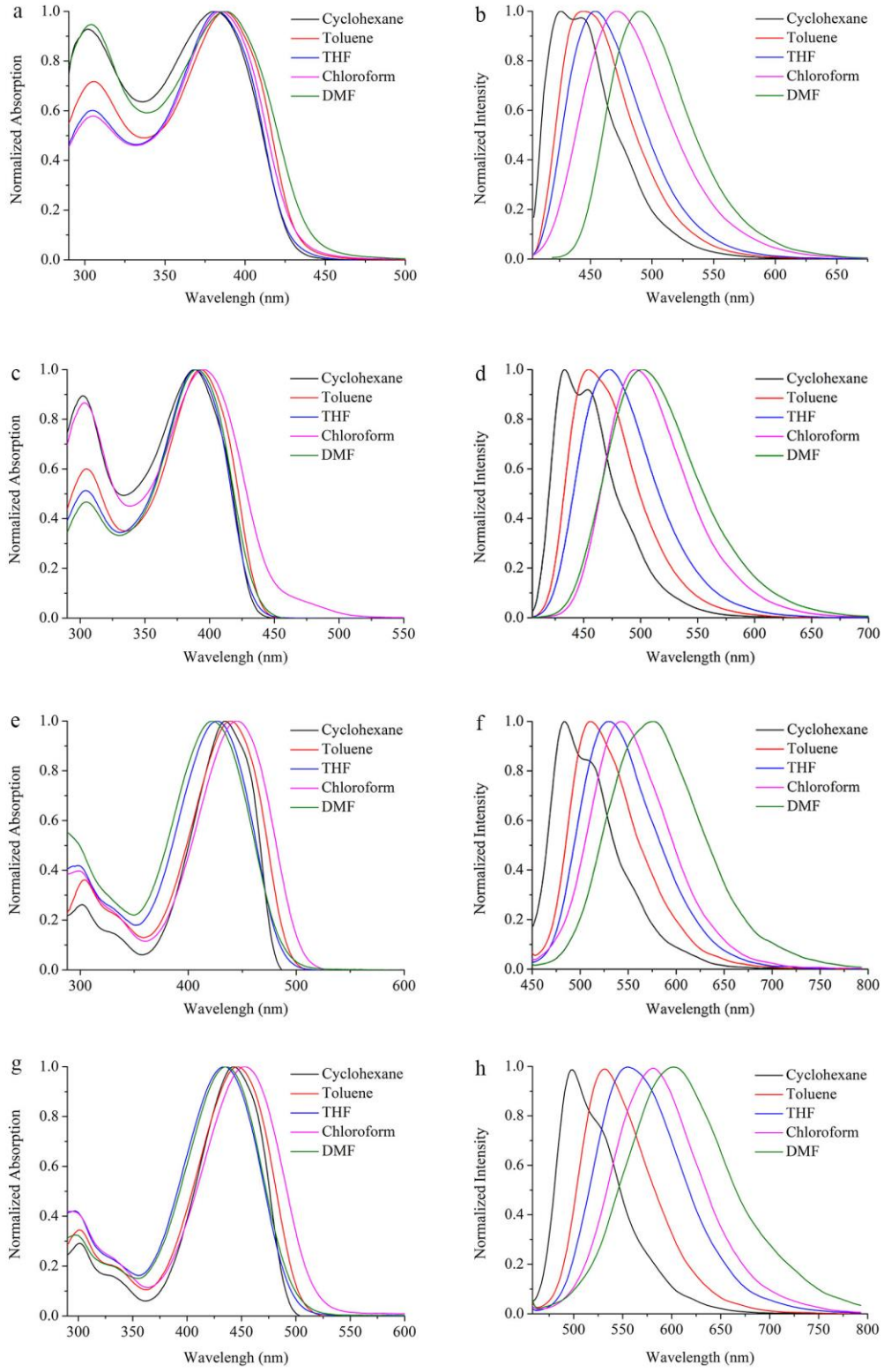

Figure S1 Normalized UV-vis absorption spectra of **BIT** (a), **BITM** (c), **BICT** (e) and **BICTM** (g) and fluorescence emission spectra of **BIT** (b, λ_{ex} = 390 nm), **BITM** (d, λ_{ex} = 390 nm), **BICT** (f, λ_{ex} = 430 nm), **BICTM** (h, λ_{ex} = 430 nm) in different solvents.

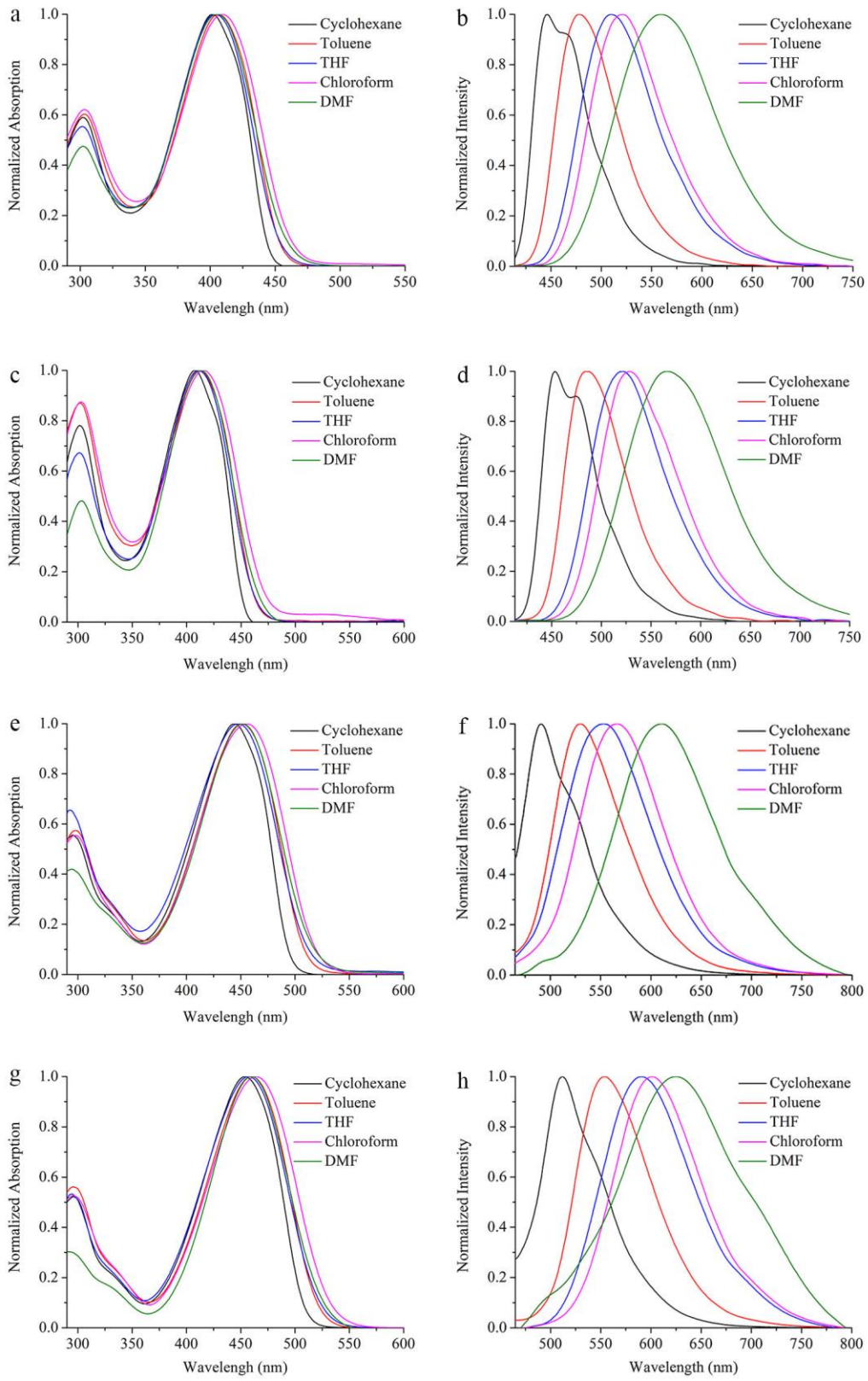

Figure S2 Normalized UV-vis absorption spectra of **BOTM** (a), **BTTM** (c), **BTCT** (e) and **BTCTM** (g) and fluorescence emission spectra of **BOTM** (b, λ_{ex} = 400 nm), **BTTM** (d, λ_{ex} = 400 nm), **BTCT** (f, λ_{ex} = 430 nm), **BTCTM** (h, λ_{ex} = 430 nm) in different solvents.

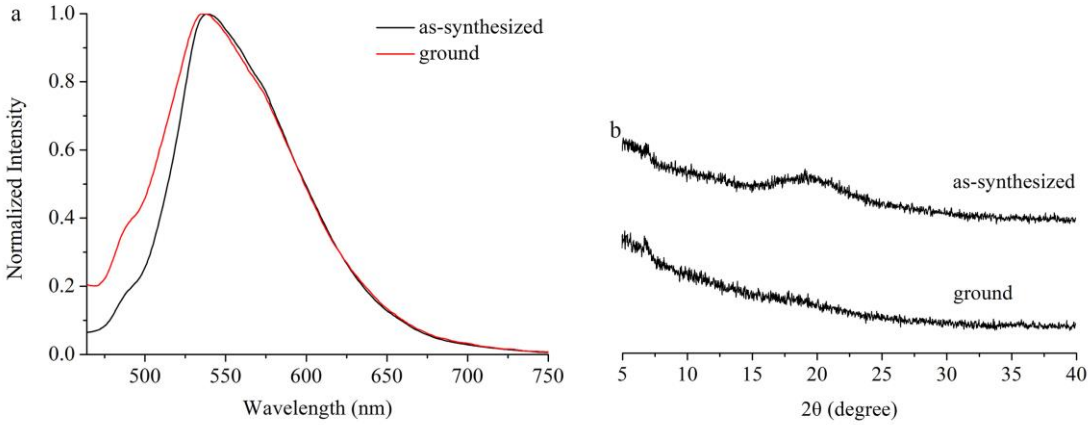

Figure S3 Normalized fluorescent emission spectra of **BIT** (a, λ_{ex} = 390 nm) and XRD patterns of **BIT** (b) in different solid-state.

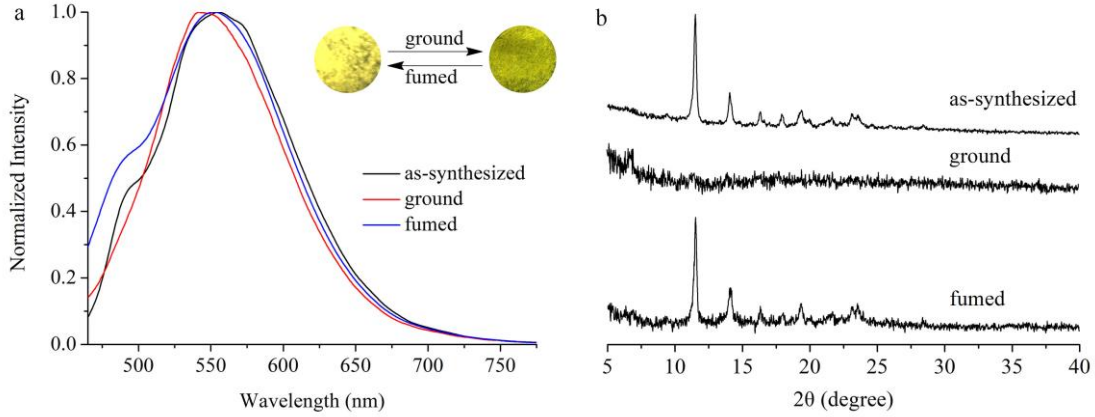

Figure S4 Normalized fluorescent emission spectra of **BITM** (a) excited at 390 nm and XRD patterns of **BITM** (b) in different solid-state.

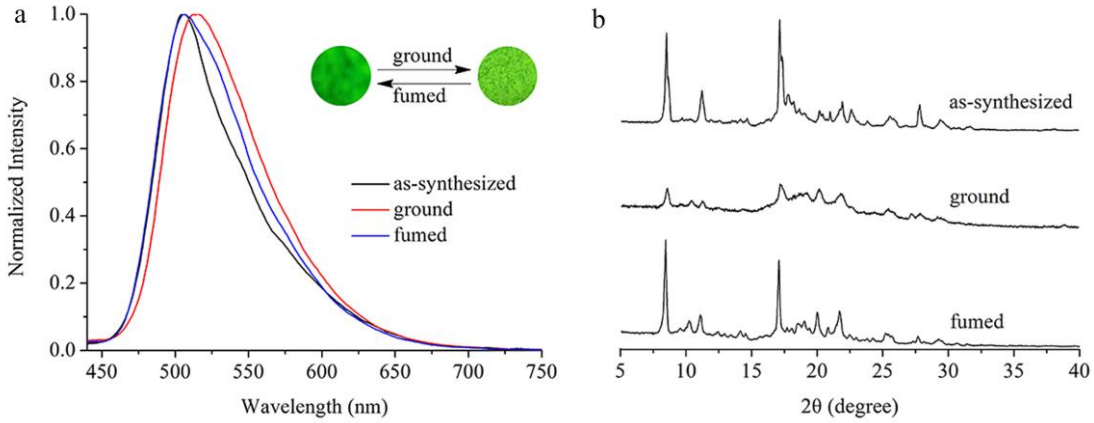

Figure S5 Normalized fluorescent emission spectra of **BOTM** (a) excited at 400 nm and XRD patterns of **BOTM** (b) in different solid-state.

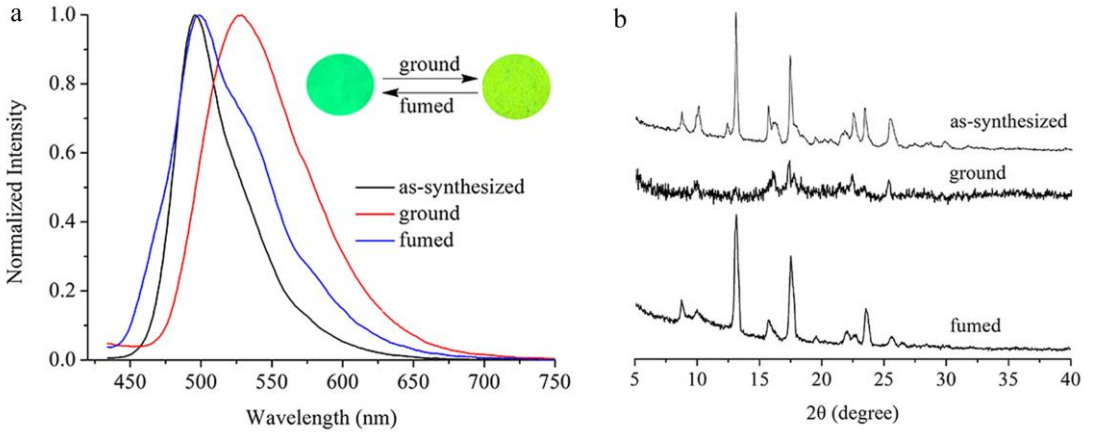

Figure S6 Normalized fluorescent emission spectra of **BTTM** (a) excited at 400 nm and XRD patterns of **BTTM** (b) in different solid-state.

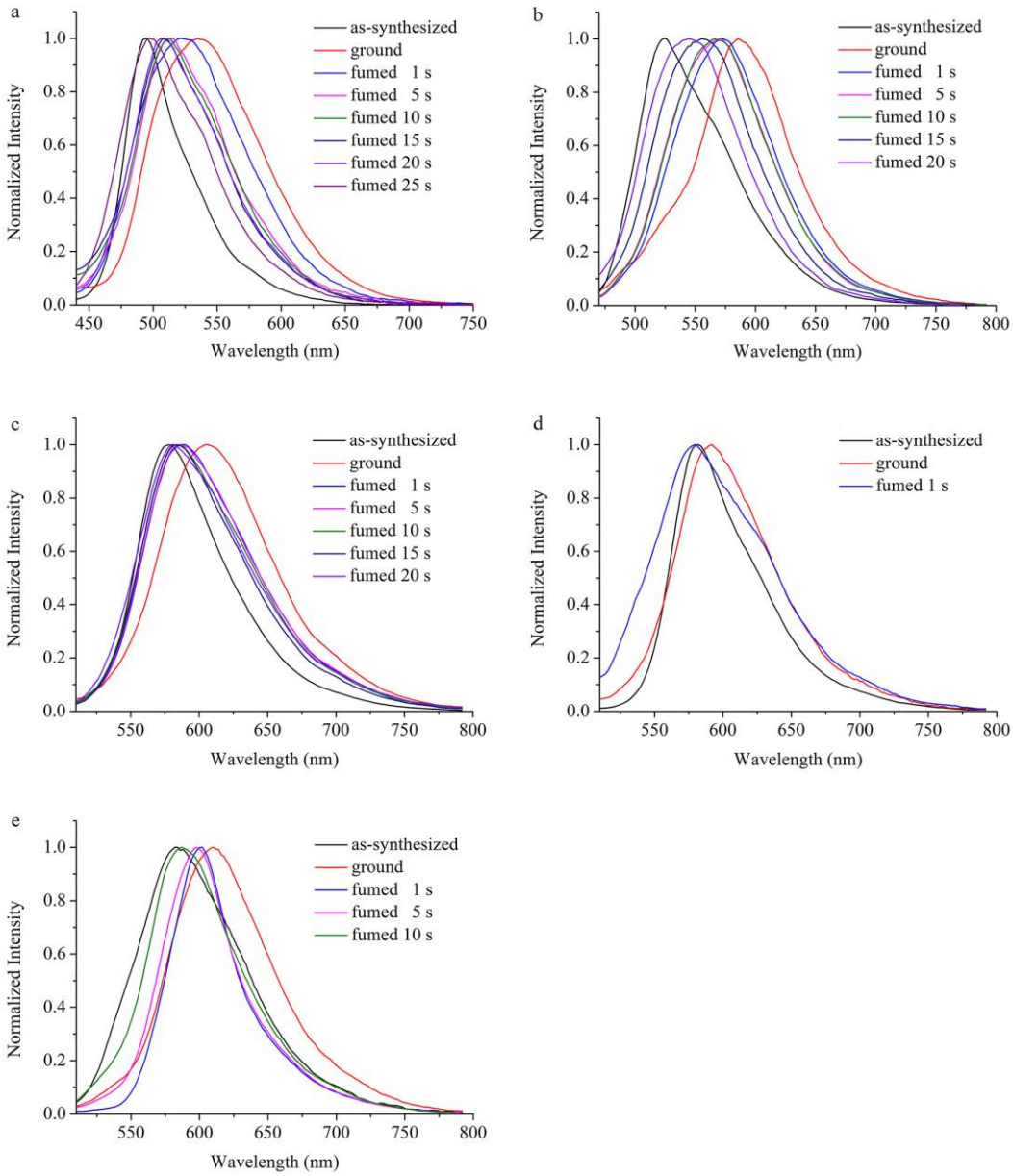

Figure S7 Fluorescence emission spectra of **BTTM** (a, λ_{ex} = 400 nm) and **BICT** (b, λ_{ex} = 430 nm), **BICTM** (c, λ_{ex} = 430 nm), **BTCT** (d, λ_{ex} = 430 nm), **BTCTM** (e, λ_{ex} = 430 nm) in the as-synthesized crystals, in the ground powders and in the fumed samples, which were prepared by fuming the ground powders with DCM for different times.

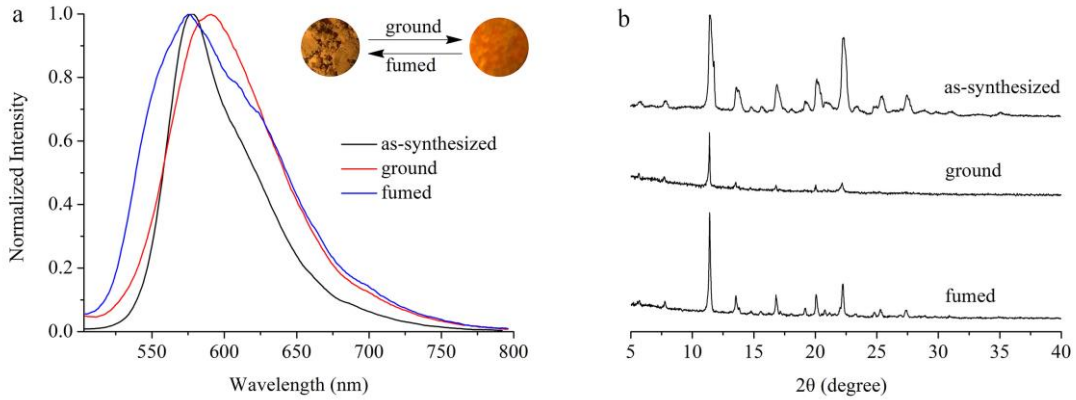

Figure S8 Normalized fluorescent emission spectra of **BTCT** (a, λ_{ex} = 430 nm) and XRD patterns of **BTCT** (b) in different solid-state.

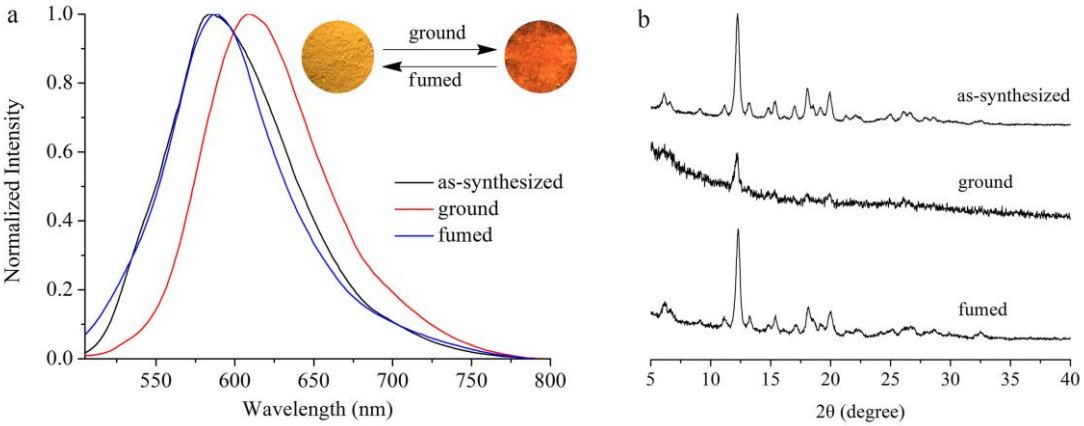

Figure S9 Normalized fluorescent emission spectra of **BTCTM** (a, λ_{ex} = 430 nm) and XRD patterns of **BTCTM** (b) in different solid-state.

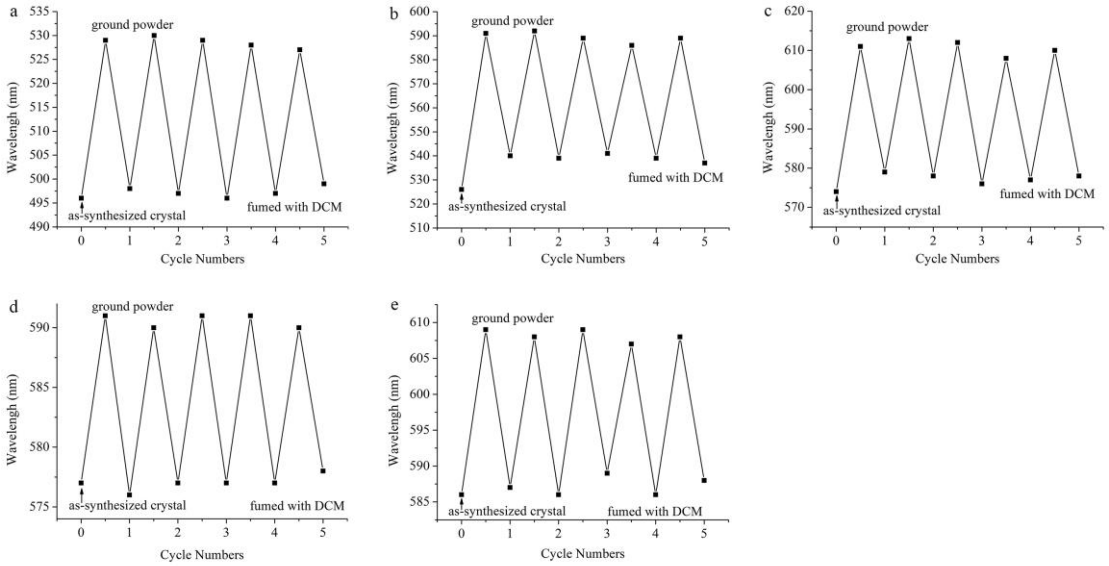

Figure S10 Maximum fluorescence emission of **BTTM** (a), **BICT** (b), **BICTM** (c), **BTCT** (d), **BTCTM** (e) upon the treatment of grinding/fuming with DCM repeatedly.

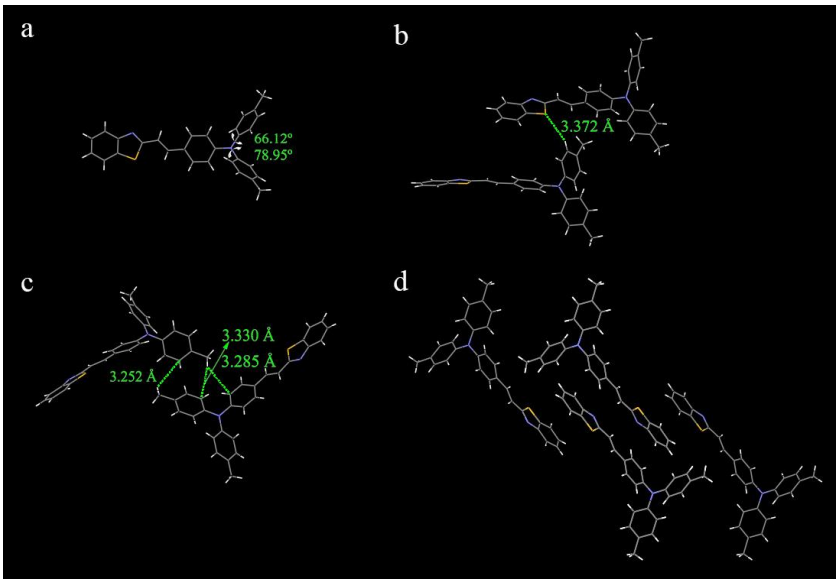

Figure S11 The molecular conformation of **BTTM** in single crystal (a); the intermolecular interactions in single crystal of **BTTM** (b, c) and single crystal structure of **BTTM** viewed along c-axis (d).

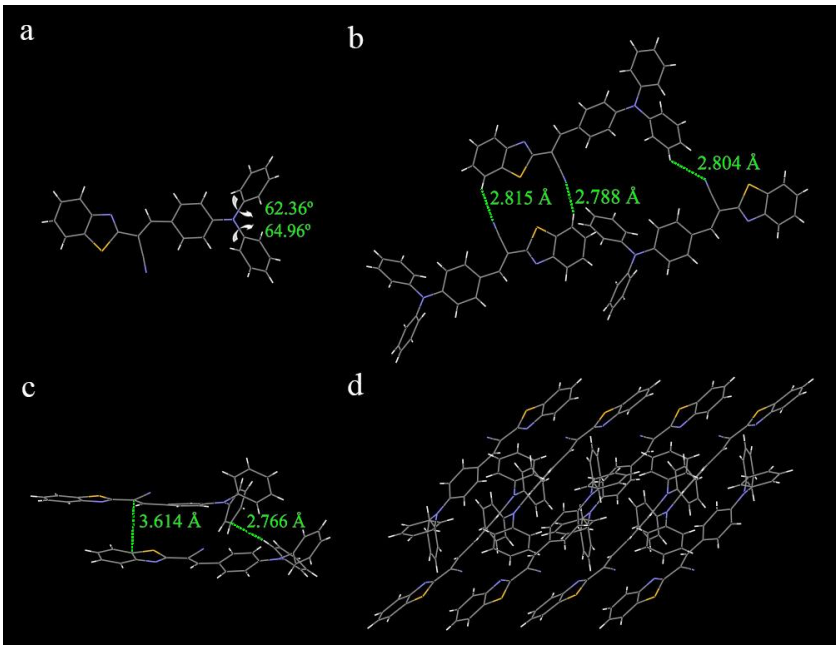

Figure S12 The molecular conformation of **BTCT** in single crystal (a); the intermolecular interactions in single crystal of **BTCT** (b, c) and single crystal structure of **BTCT** viewed along b-axis (d).

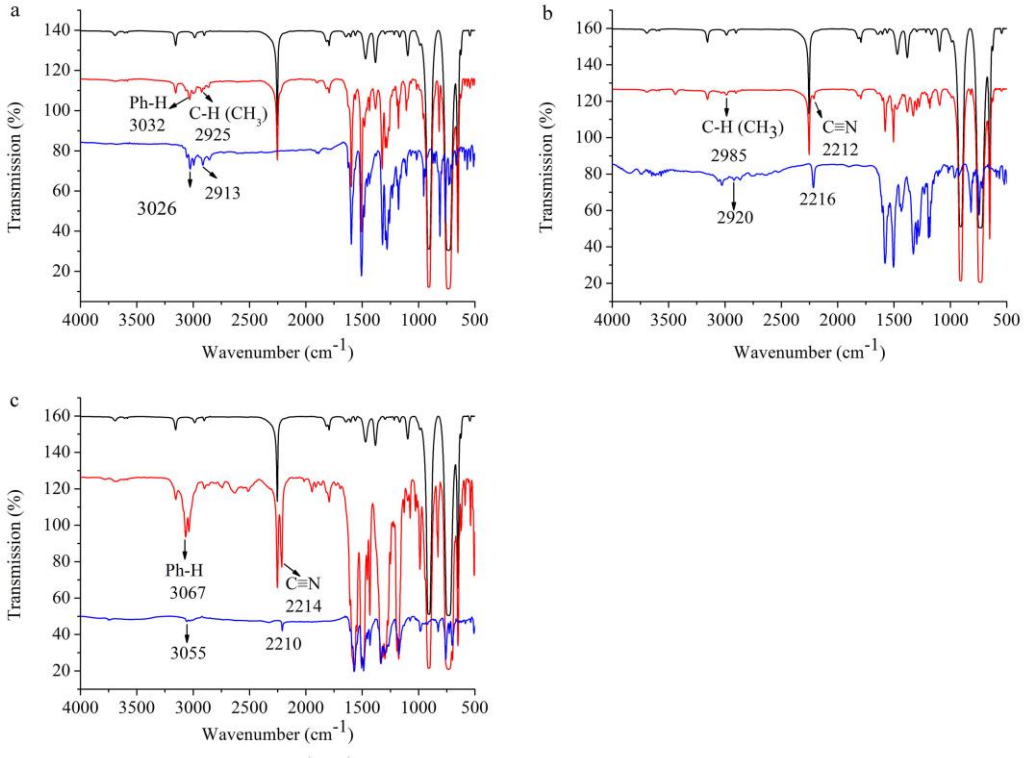

Figure S13 FT-IR spectra of **BTTM** (a), **BICTM** (b) and **BTCT** (c) in $CDCl_3$ (red) and in crystals (blue); FT-IR spectra of $CDCl_3$ containing TMS (black).

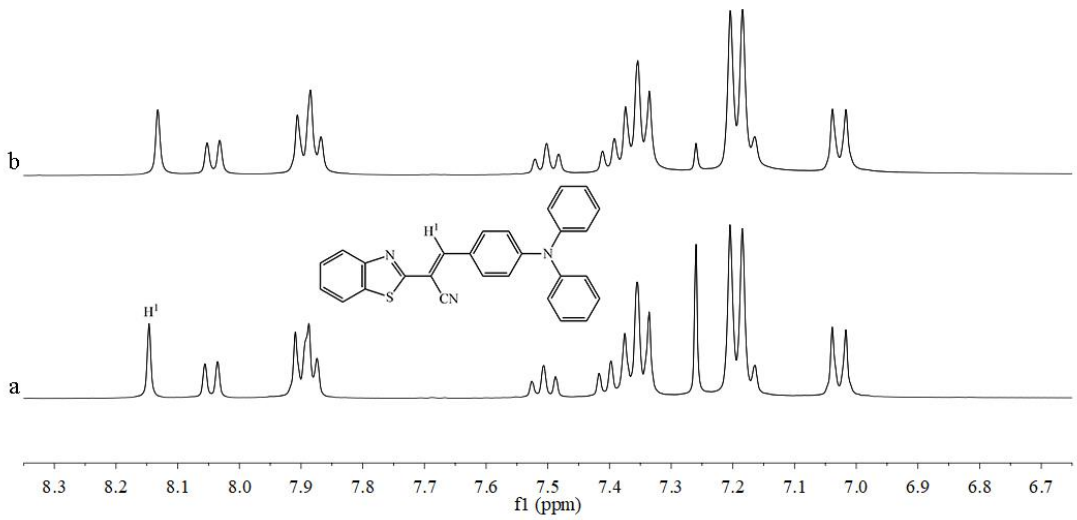

Figure S14 ^{1}H NMR (400 MHz) spectrum of **BTCT** in $CDCl_3$ (a: 8 mg/mL, b: 33 mg/mL).

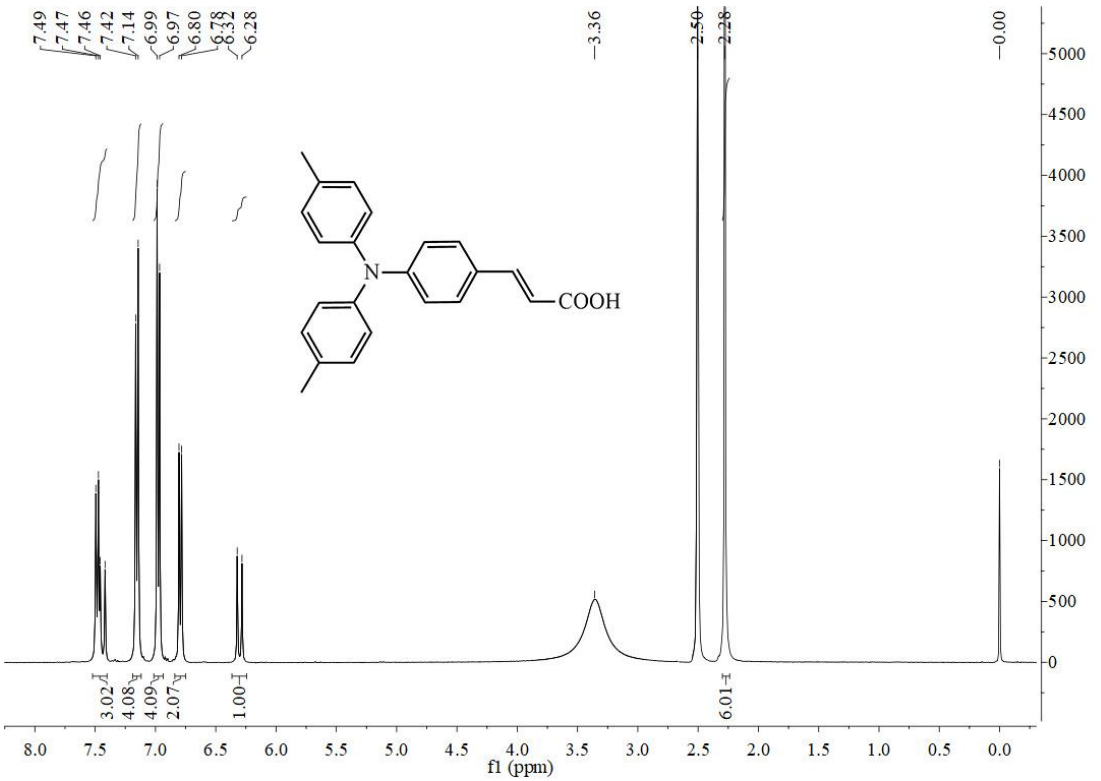

Figure S15 ^{1}H NMR (400 MHz) spectrum of (*E*)-3-(4-(di*p*-tolylamino)phenyl)acrylic acid in DMSO-d_6.

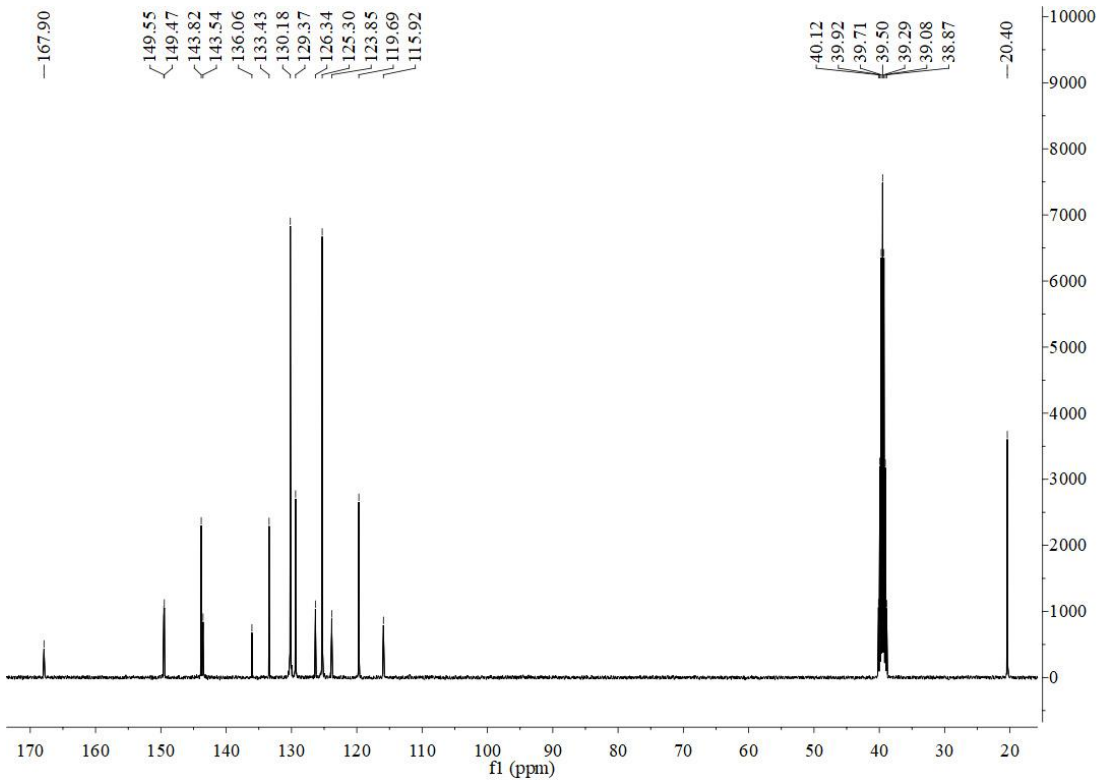

Figure S16 ^{13}C NMR (101 MHz) spectrum of (*E*)-3-(4-(di*p*-tolylamino)phenyl)acrylic acid in DMSO-d_6.

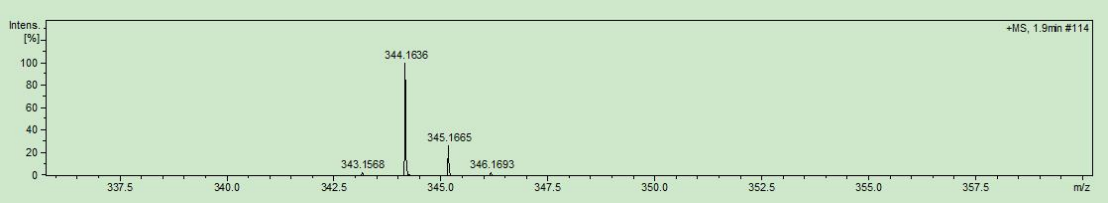

Figure S17 The HRMS of (*E*)-3-(4-(di*p*-tolylamino)phenyl)acrylic acid.

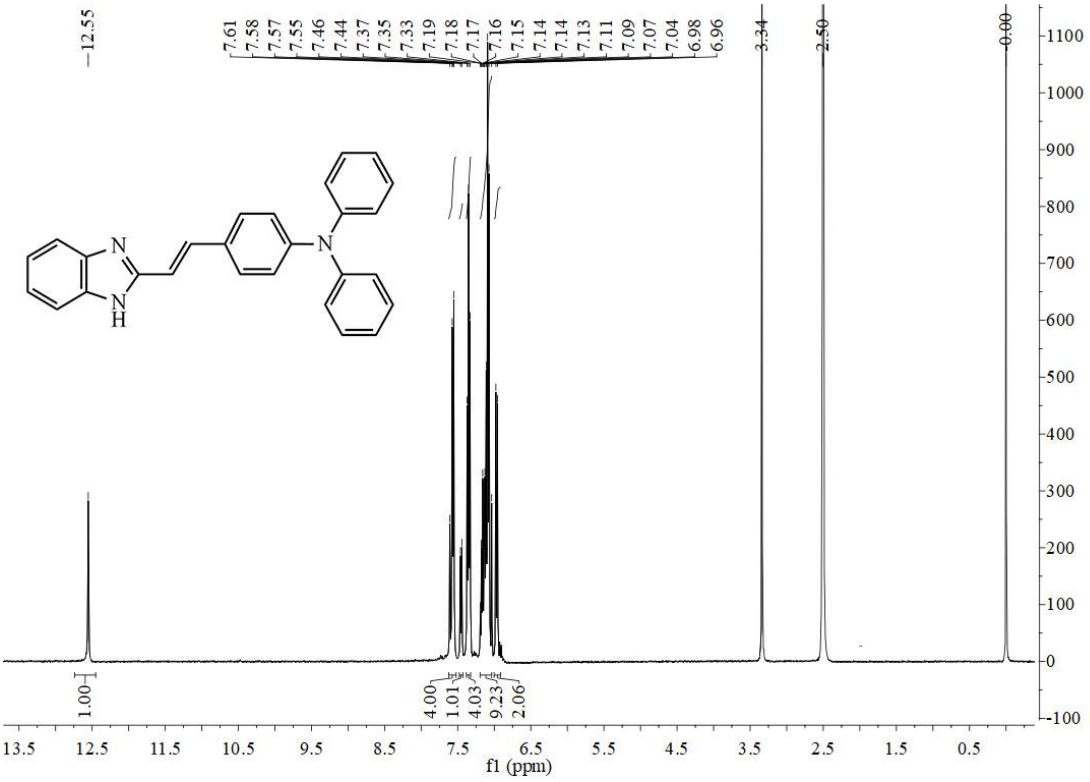

Figure S18 ^{1}H NMR (400 MHz) spectrum of **BIT** in DMSO-d_6.

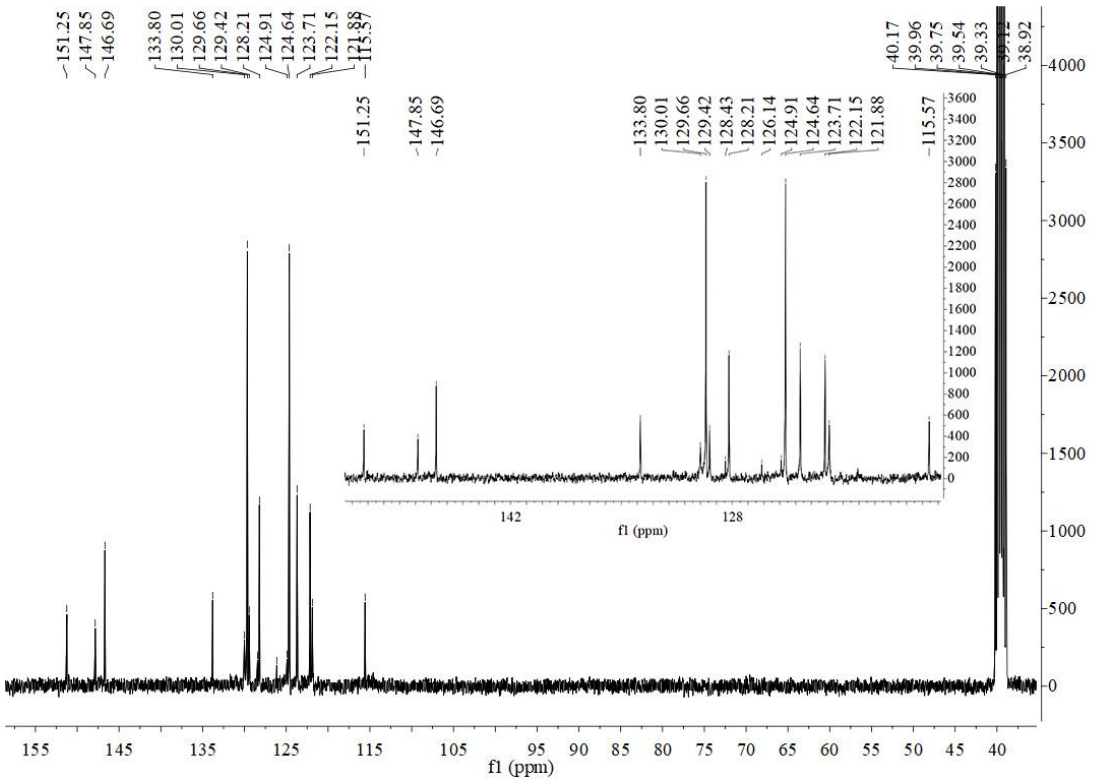

Figure S19 ^{13}C NMR (101 MHz) spectrum of **BIT** in DMSO-d_6.

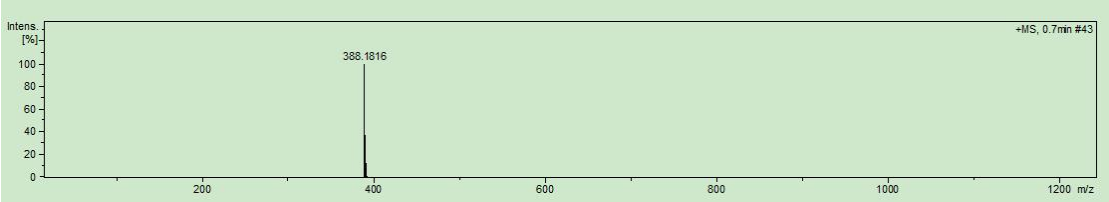

Figure S20 The HRMS of **BIT**.

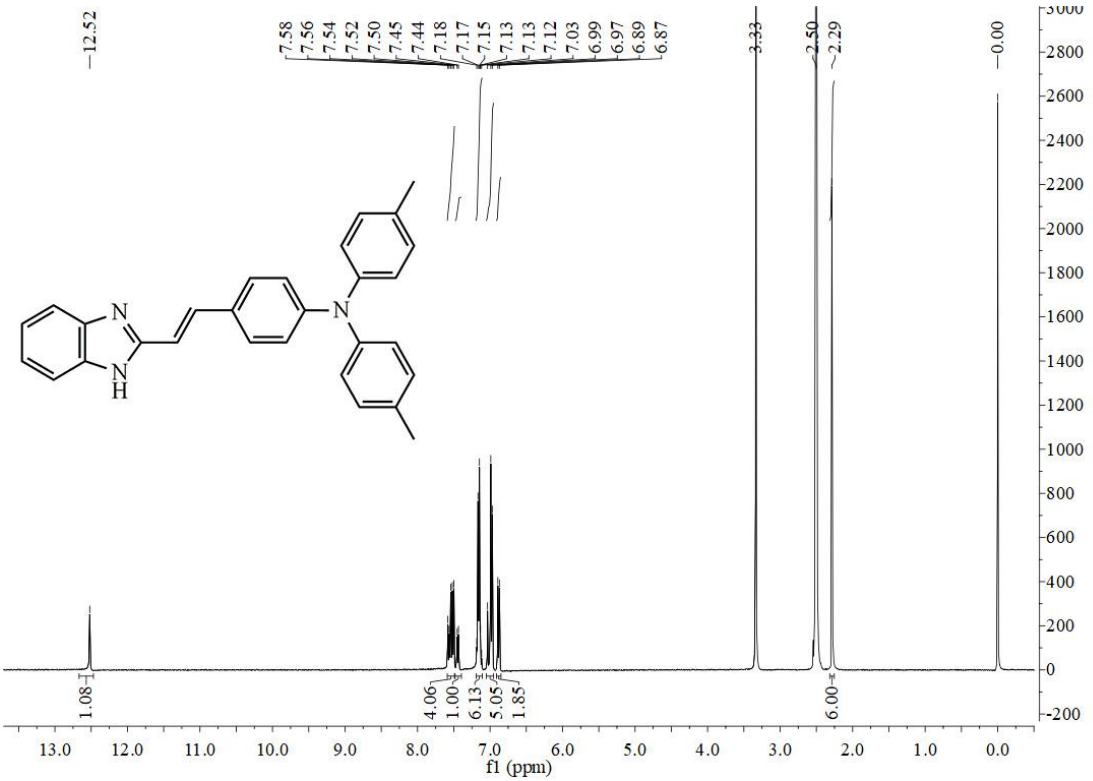

Figure S21 ^{1}H NMR (400 MHz) spectrum of **BITM** in DMSO-d_6.

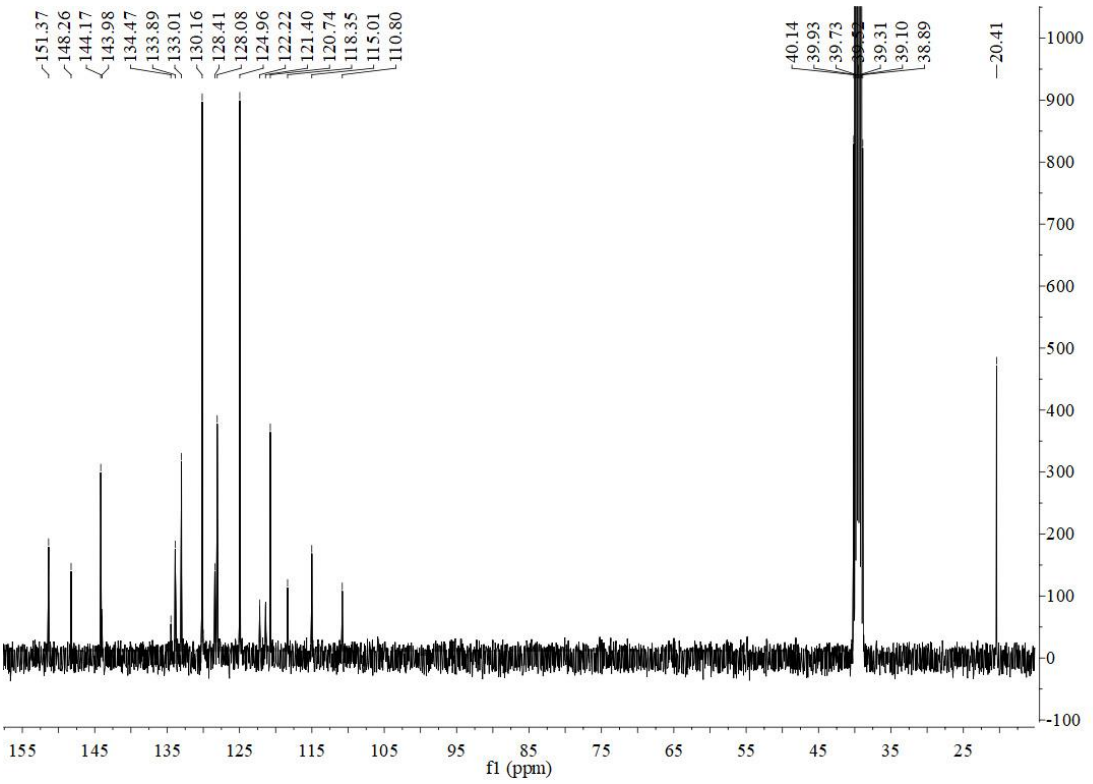

Figure S22 ^{13}C NMR (101 MHz) spectrum of **BITM** in DMSO-d_6.

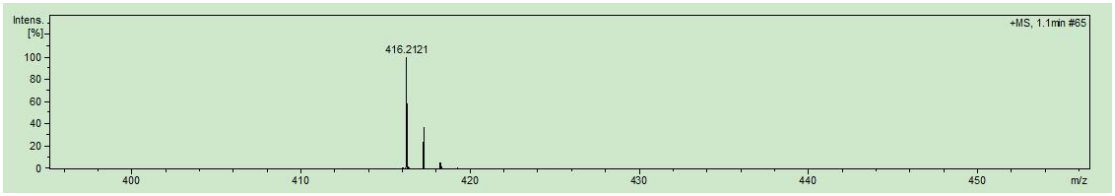

Figure S23 The HRMS of **BITM**.

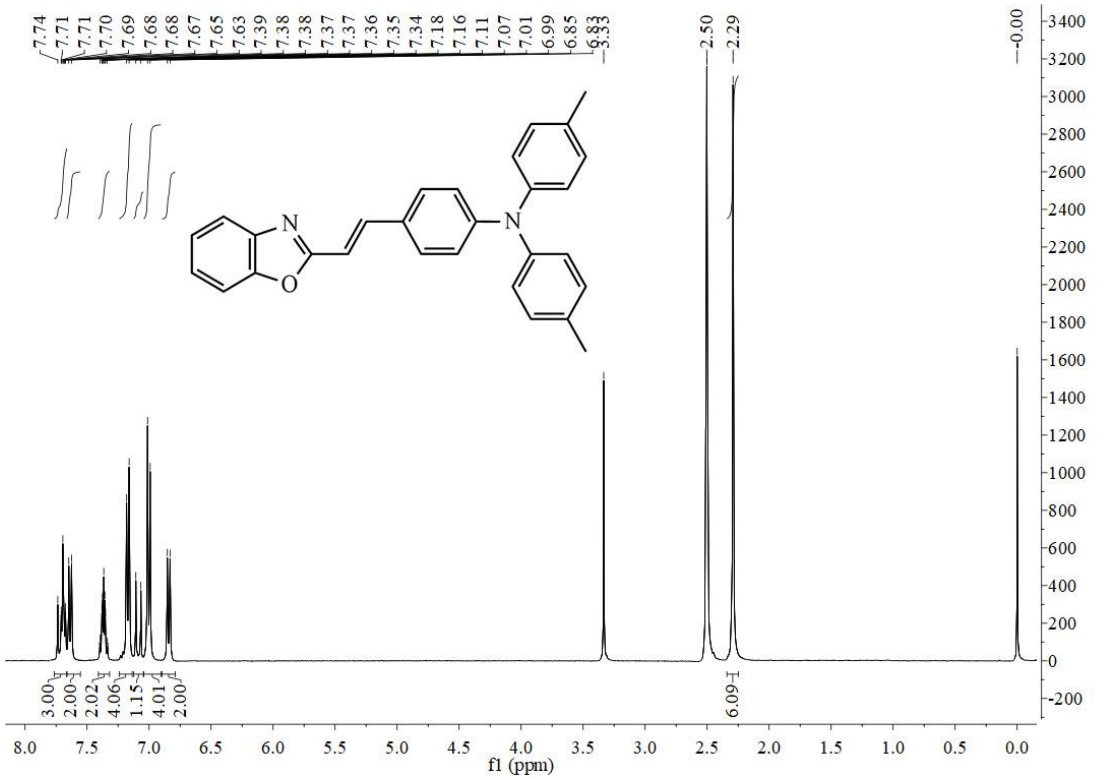

Figure S24 ^{1}H NMR (400 MHz) spectrum of **BOTM** in DMSO-d_6.

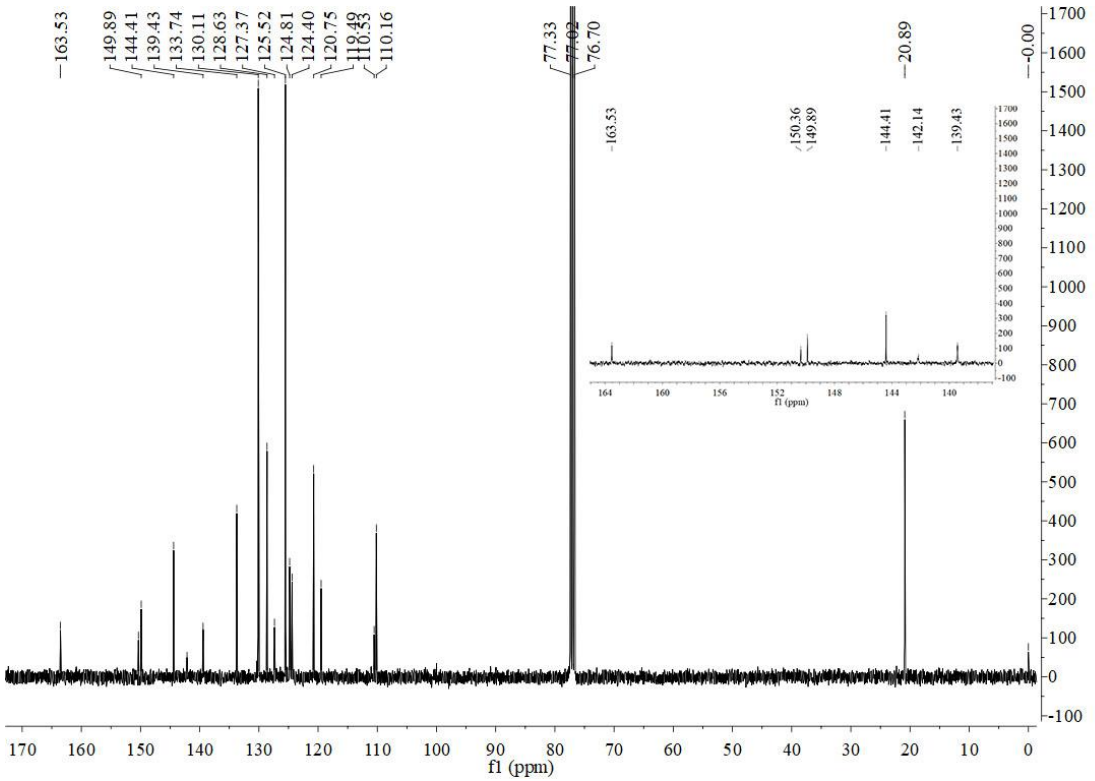

Figure S25 ^{13}C NMR (101 MHz) spectrum of **BOTM** in $CDCl_3$.

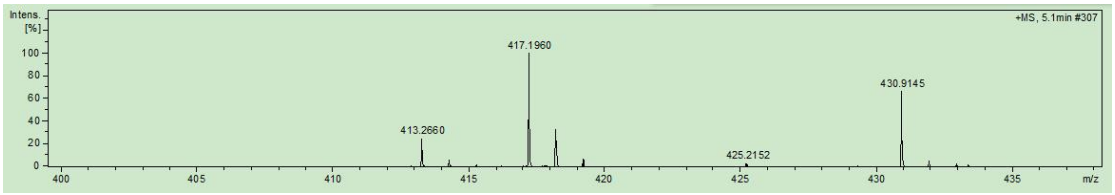

Figure S26 The HRMS of **BOTM**.

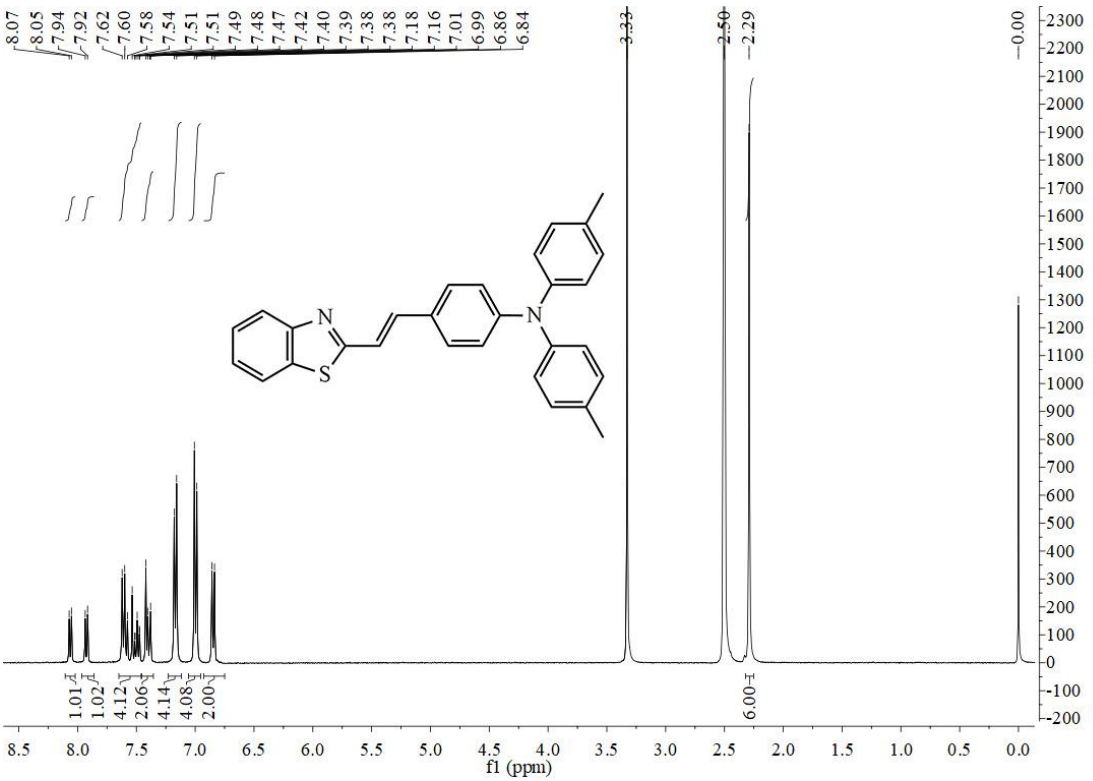

Figure S27 ^{1}H NMR (400 MHz) spectrum of **BTTM** in DMSO-d_6.

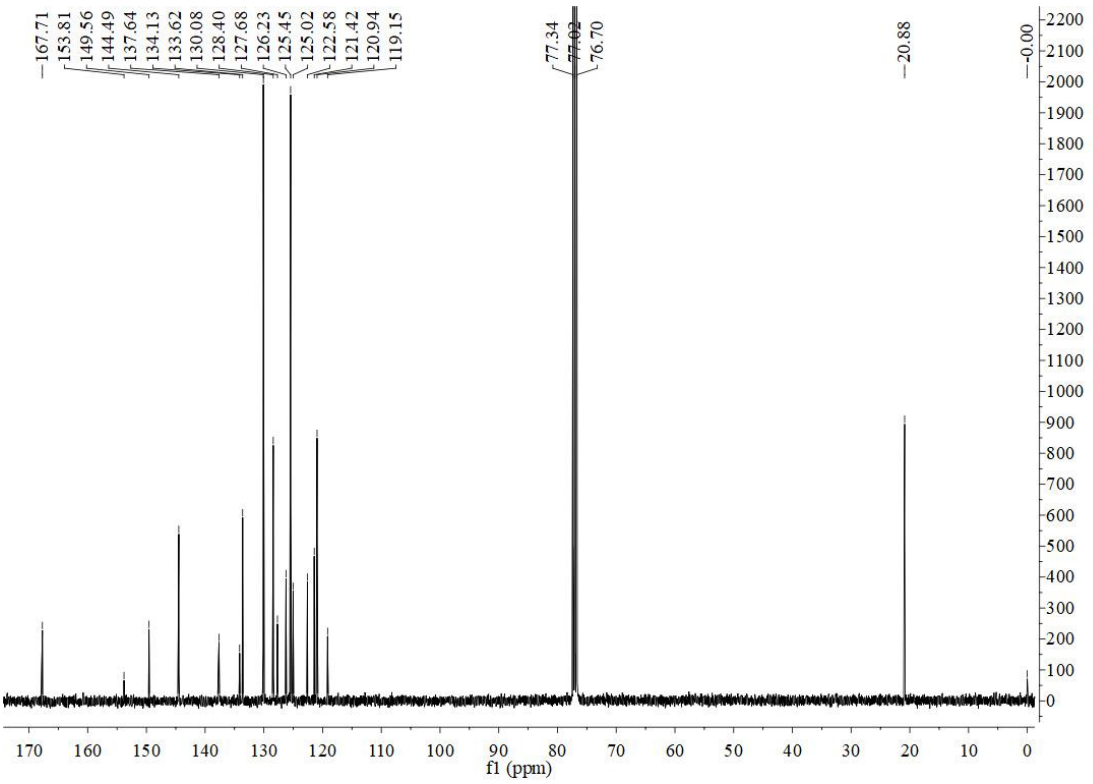

Figure S28 ^{13}C NMR (101 MHz) spectrum of **BTTM** in $CDCl_3$.

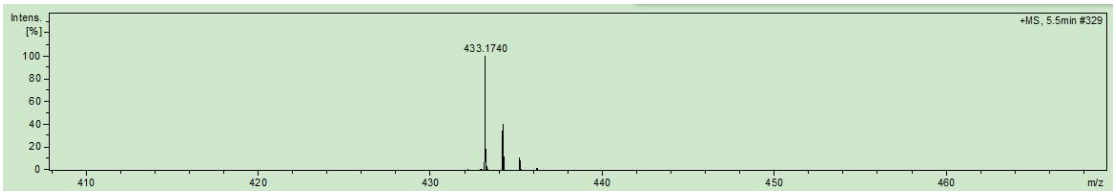

Figure S29 The HRMS of **BTTM**.

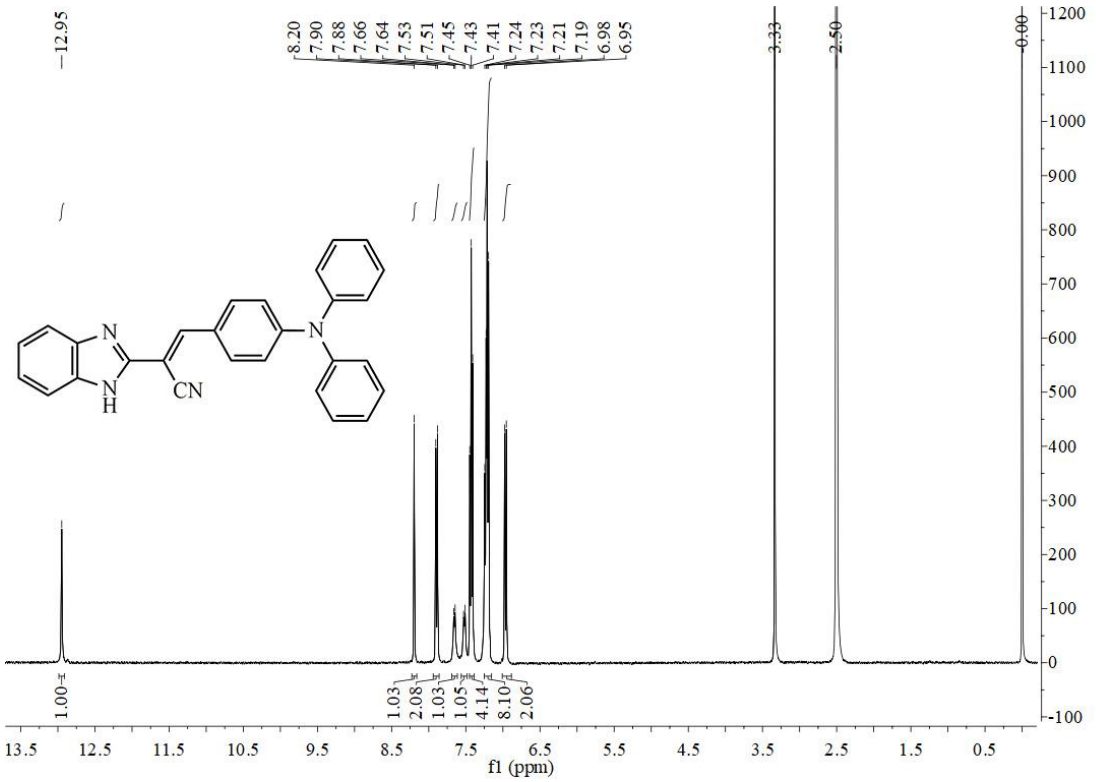

Figure S30 ^{1}H NMR (400 MHz) spectrum of **BICT** in DMSO-d_6.

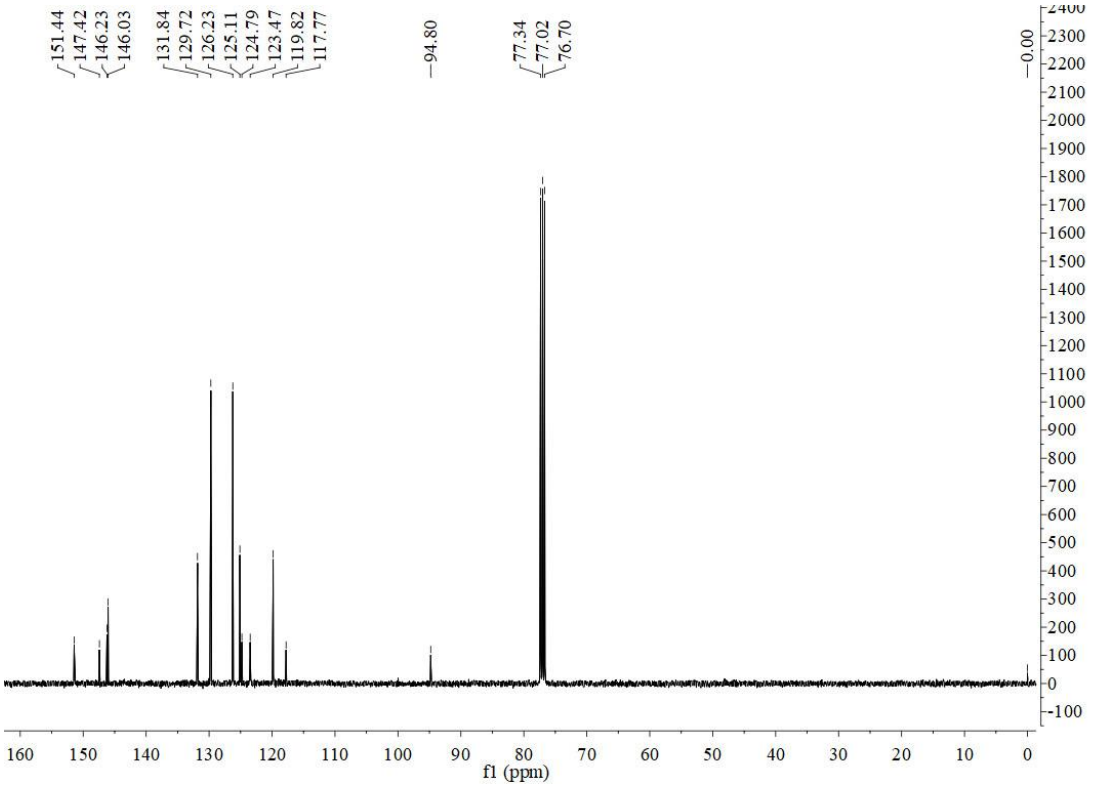

Figure S31 ^{13}C NMR (101 MHz) spectrum of **BICT** in $CDCl_3$.

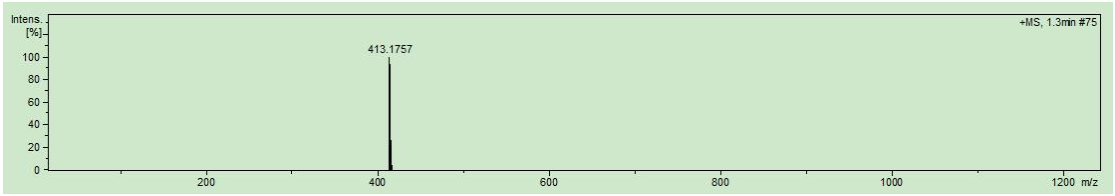

Figure S32 The HRMS of **BICT**.

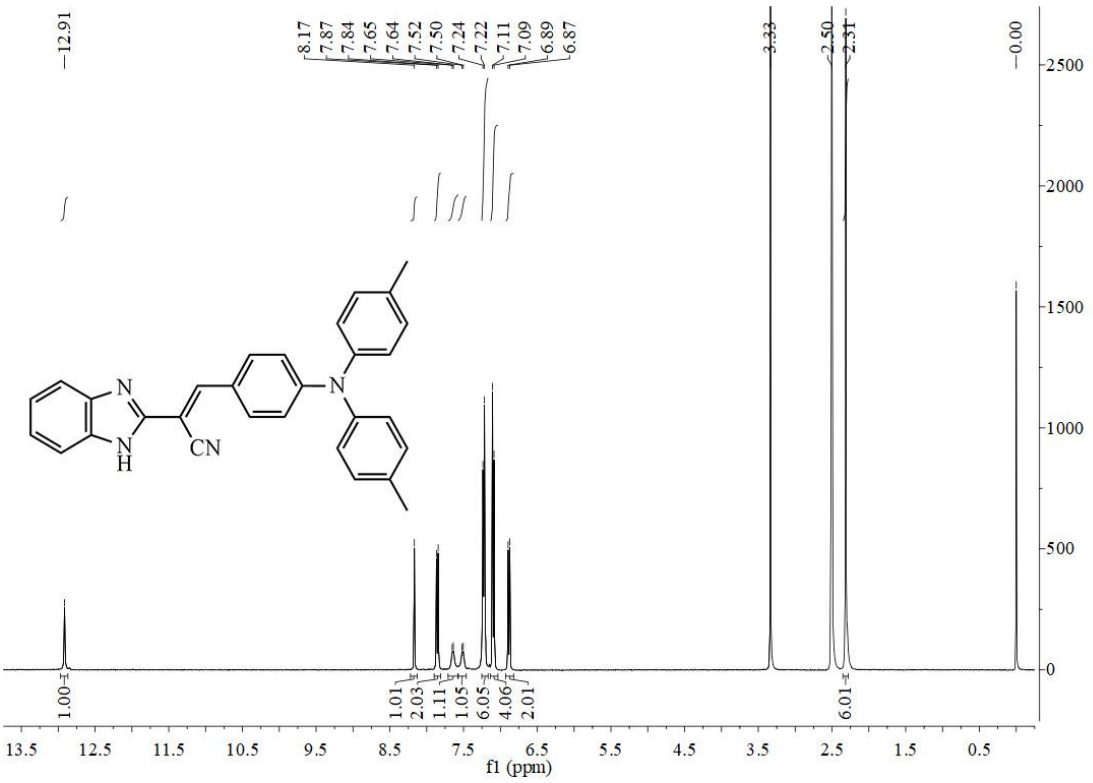

Figure S33 ^{1}H NMR (400 MHz) spectrum of **BICTM** in DMSO-d_6.

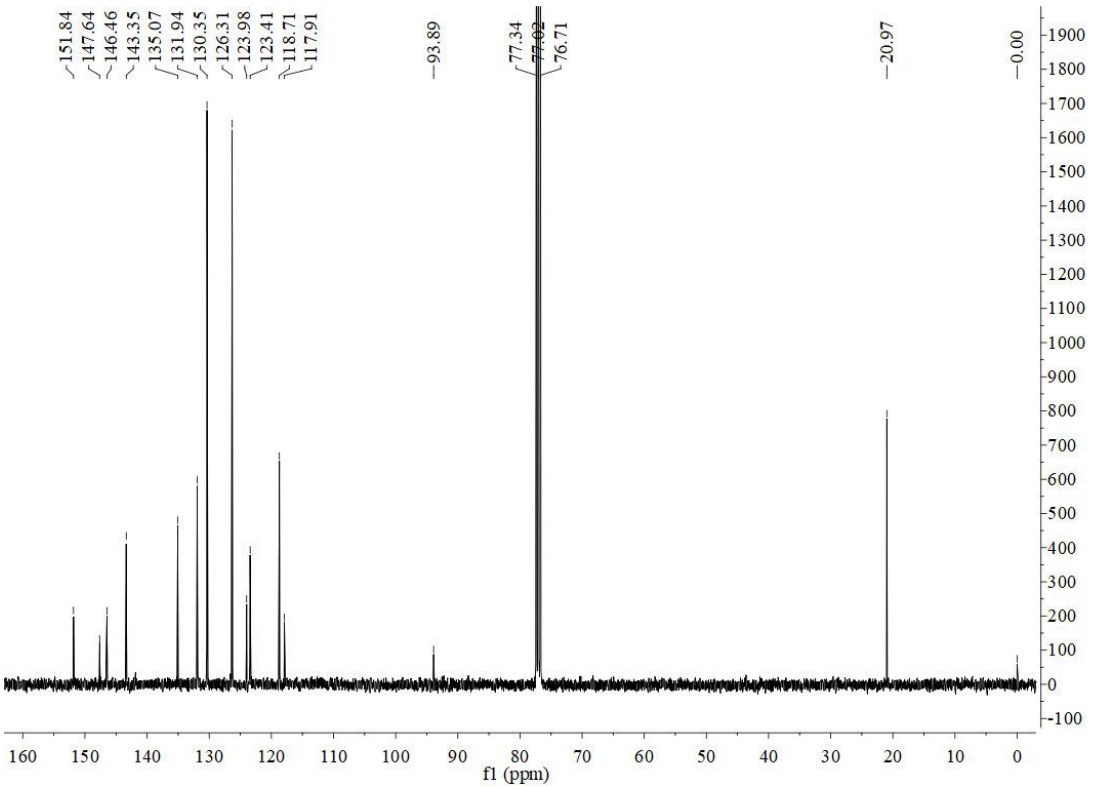

Figure S34 ^{13}C NMR (101 MHz) spectrum of **BICTM** in $CDCl_3$.

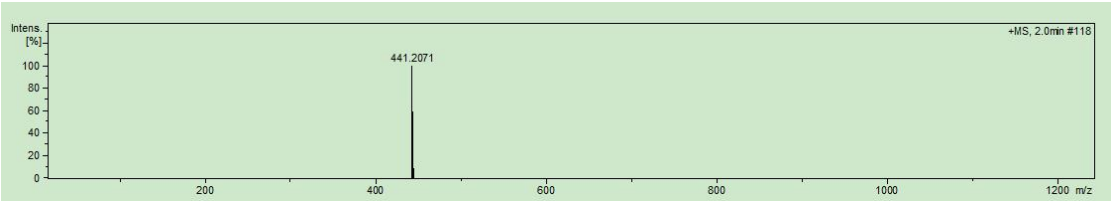

Figure S35 The HRMS of **BICTM**.

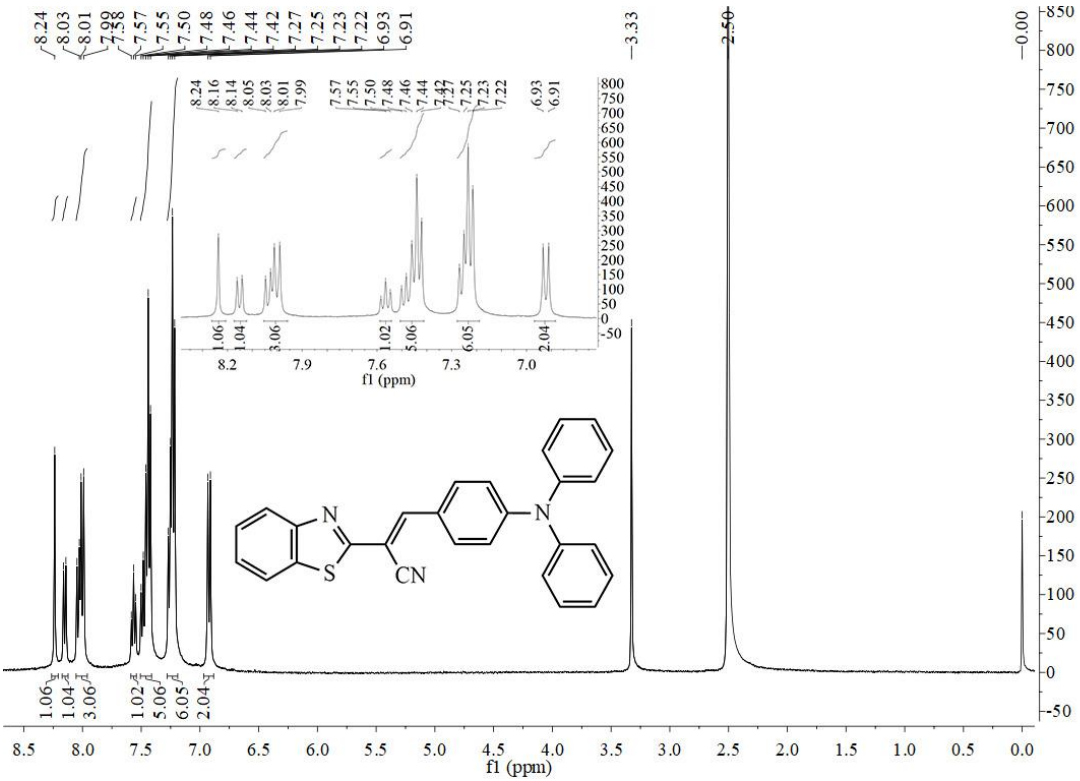

Figure S36 ^{1}H NMR (400 MHz) spectrum of **BTCT** in DMSO-d_6.

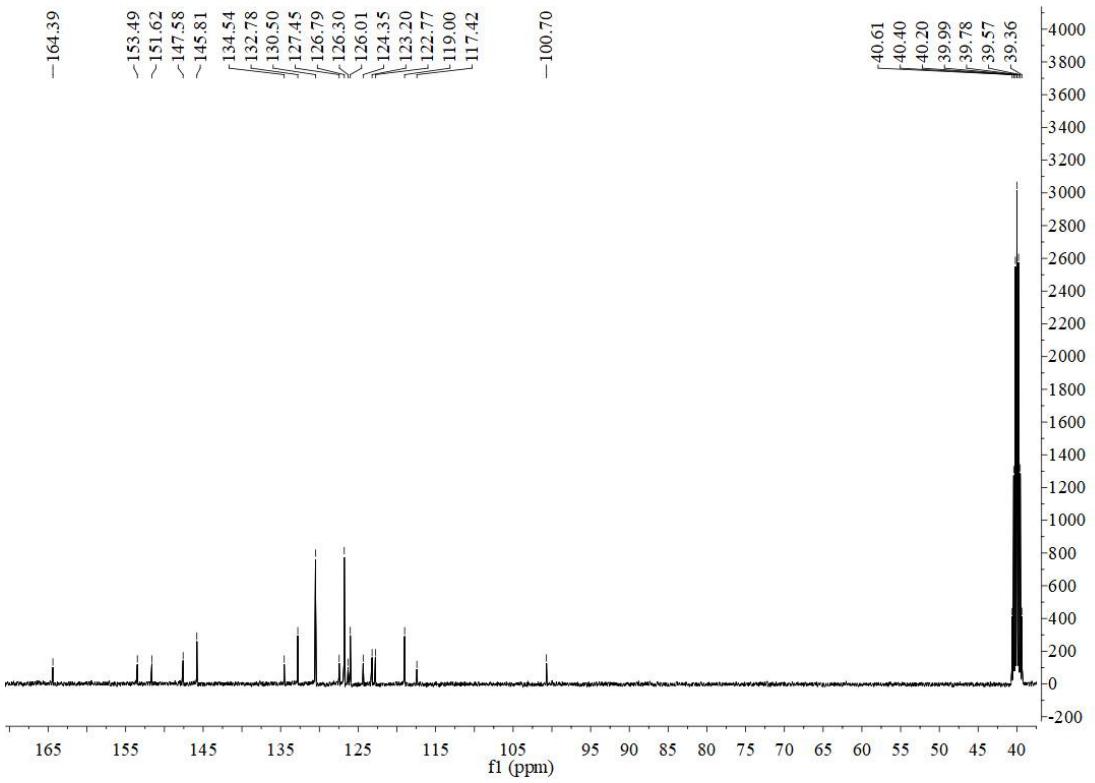

Figure S37 ^{13}C NMR (101 MHz) spectrum of **BTCT** in DMSO-d_6.

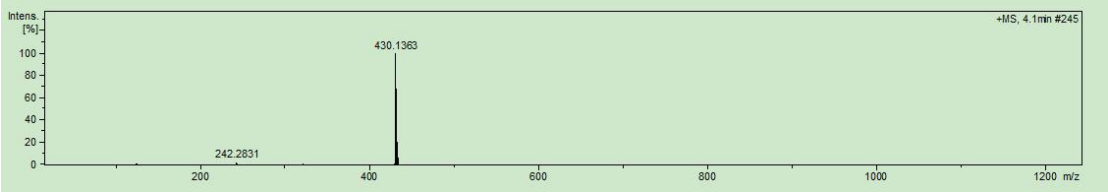

Figure S38 The HRMS of **BTCT**.

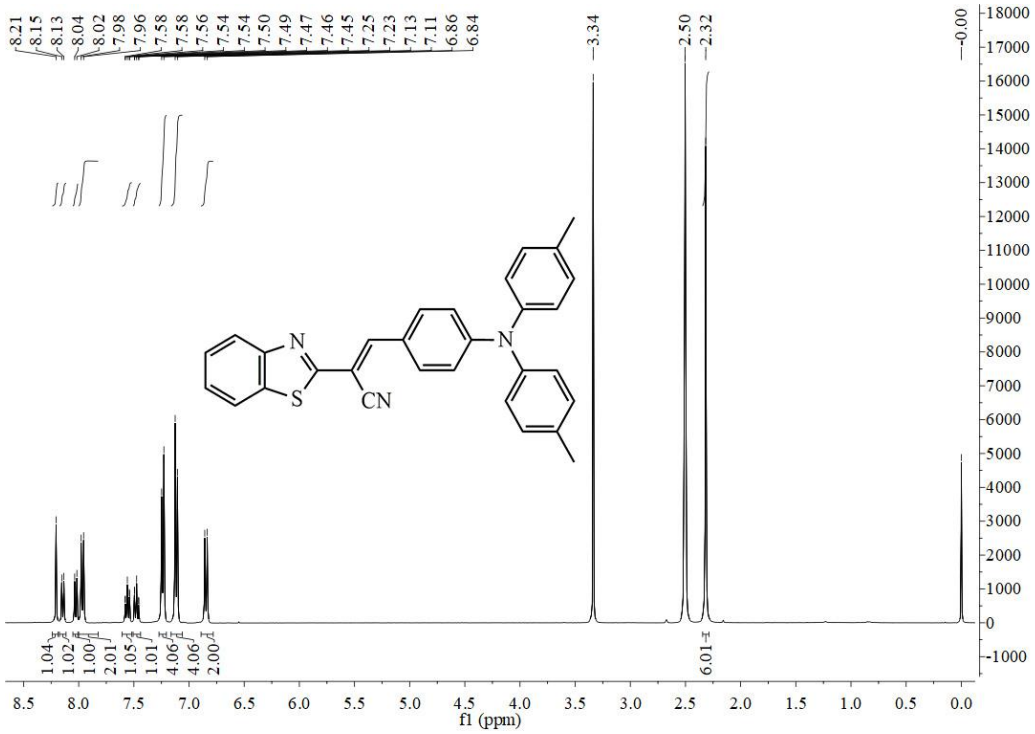

Figure S39 ^{1}H NMR (400 MHz) spectrum of **BTCTM** in DMSO-d_6.

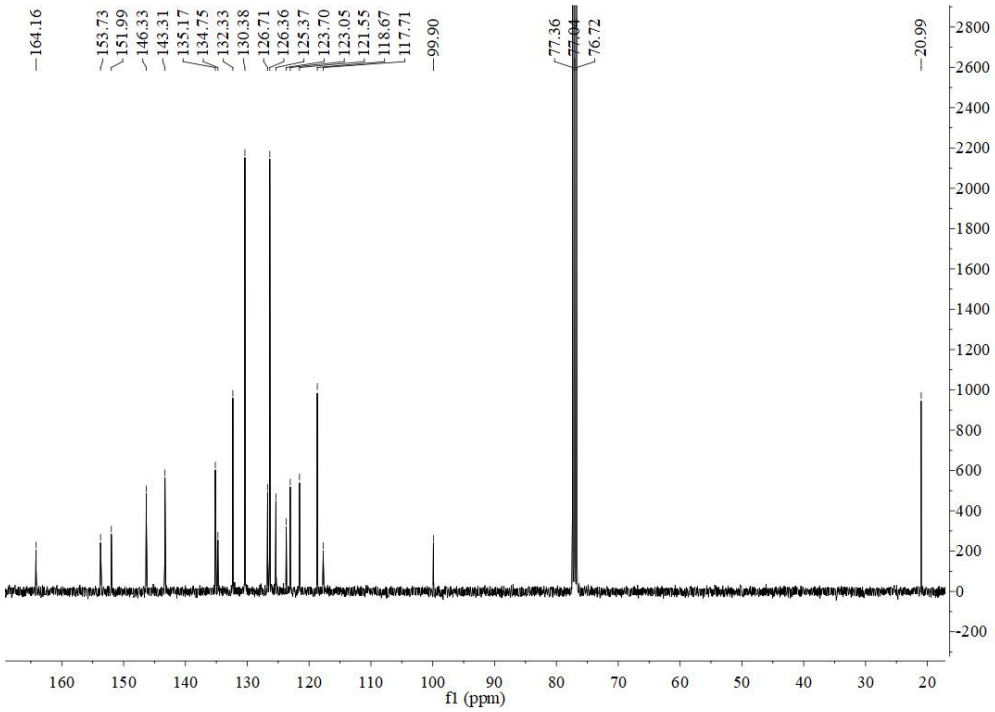

Figure S40 ^{13}C NMR (101 MHz) spectrum of **BTCTM** in $CDCl_3$.

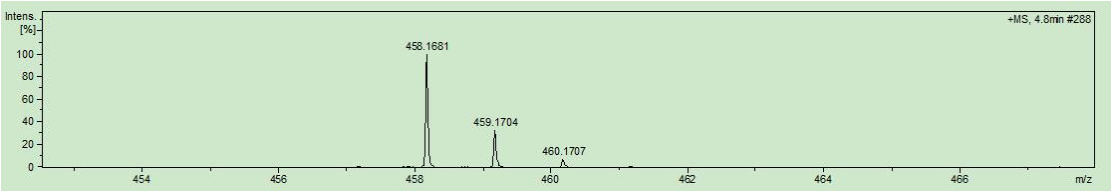

Figure S41 The HRMS of **BTCTM**.